Decay of Ni^{56}†

D. O. WELLS,* S. L. BLATT, AND W. E. MEYERHOF
Stanford University, Stanford, California
(Received 31 January 1963)

The radioactive decay of Ni^{56} to Co^{56} (half-life remeasured, 6.10±0.02 days) has been investigated using scintillation gamma-ray spectrometers, both singly and in coincidence. The spectra revealed gamma rays of 0.164±0.003(99.3±6.6), 0.272±0.004(31.5±5.2), 0.484±0.004(34.6±2.0), 0.755±0.003(48.0±3.2), 0.820±0.003(84.9±8.3), 0.982±0.010(1.2±0.1), and 1.57±0.01(14.1±0.9) MeV. The intensities of the gamma rays (number per 100 decays) appear in parentheses. The data were consistent with an upper limit of 1 per 100 decays for the intensity of any positron emission. Coincidence spectra, angular-correlation measurements, and delayed-coincidence measurements permitted the construction of a decay scheme with energy levels at 0.00(4^+), 0.164(3^+), 0.984(2^+), 1.47(1^-,$2^\pm$), and 1.74(1^+) MeV. The level scheme is compared with other recent work concerning the energy levels of Co^{56}.

I. INTRODUCTION

THE energy levels of Co^{56} should provide a good test for the applicability of the nuclear shell model in the region of the periodic table near $A=56$, for its 27 protons and 29 neutrons are both but one removed from the magic number 28. The first attempt to study the levels of Co^{56} populated through the decay of Ni^{56} was made by Sheline and Stoughton.[1] They found gamma rays of 0.17 (100), 0.28 (30), 0.48 (40), 0.81 (80), 0.96 (10), 1.33 (5), 1.58 (15), and 1.75 (2) MeV (numbers in parentheses indicate relative intensities). A value of 6.4±0.1 days was measured for the half-life of the decay and an upper limit of 0.01 was placed on the fractional intensity of any positron emission. An upper limit of 10^{-4} was obtained for any alpha branching ratio for the decay. Worthington[2] found evidence for the presence of Ni^{56} among the high-energy spallation products of zinc bombarded by 340-MeV protons. He measured a decay half-life of 6.0±0.5 days and observed gamma rays of 0.16, (0.25), 0.5, 0.8, and $\gtrsim$1.4 MeV. A thorough study of the decay scheme was not attempted. Wilkinson and Sheline,[3,4] using more modern electronic equipment and larger gamma-ray detectors, observed gamma rays of 0.161 (100), 0.261 (30), 0.462 (40), 0.750 (50), 0.845 (90), 0.950 (50), 1.33 (3), 1.58 (4), and 1.74 (2) MeV. They also measured gamma-gamma coincidences. A satisfactory decay scheme was not constructed from any of the above experiments.

The magnetic moment and spin of the ground state of Co^{56} have been measured in several experiments.[5,6] Direct measurements by paramagnetic resonance studies led to absolute values for the magnetic moment of[7] 3.855±0.007 and[8] 3.848±0.015 nm and for the spin of four. The parity of the ground state has been assumed to be positive on the basis of the shell model.

The work reported here was an attempt to obtain a consistent decay scheme for the decay of Ni^{56} to Co^{56} using scintillation spectrometers both singly and in coincidence.

II. SOURCE PREPARATION

Ni^{56} was produced via the $Fe^{54}(\alpha,2n)Ni^{56}$ reaction by bombarding spectrographically standardized natural iron foils with alpha particles in the internal beam of the 60-in. cyclotron at the Crocker Laboratory of the University of California. The alpha particles, which are normally 45 MeV, were degraded to 30 MeV by inserting 0.019 in. of aluminum in front of the target. The iron foils were 0.0035 to 0.0040 in. thick. (This represents an energy loss of about 10 MeV for 30-MeV alpha particles.) The total integrated beam currents used in the bombardments ranged from 150 to 300 μAh. The maximum beam amplitude which could be tolerated was about 23 μA. One to two weeks were allowed to elapse after the bombardments so that short-lived activities could decay. The Ni^{56} was then chemically separated from the iron and the other reaction products by the methods of solvent extraction and anion-exchange columns.

In a few of the first experiments, 45-MeV alpha particles and 0.018-in.-thick targets were used. Bombardment at this energy produced Mn^{52} and Mn^{54} by the $Fe^{54}(\alpha,\alpha'pn)Mn^{52}$ and $Fe^{56}(\alpha,\alpha'pn)Mn^{54}$ reactions.[9] The presence of a Mn^{52} contamination in the source was quite serious, since the similarity of the half-lives of Mn^{52} and Ni^{56} (5.72 days[10] and 6.10 days, respectively) made identification of their specific radiations impos-

† Supported in part by the joint program of the Office of Naval Research and the U. S. Atomic Energy Commission. Material summarized from the Ph.D. thesis of D. O. Wells, Stanford University, 1962 (unpublished).
* Present address; the Department of Physics, University of Oregon, Eugene, Oregon.
[1] R. K. Sheline and R. W. Stoughton, Phys. Rev. **87**, 1 (1952).
[2] W. J. Worthington, Phys. Rev. **87**, 158L (1952).
[3] J. R. Wilkinson (private communication).
[4] J. R. Wilkinson and R. K. Sheline (private communication quoted in *Nuclear Data Sheets*, $A=56$).
[5] L. J. Gallaher, Ch. Wittle, J. A. Beun, A. N. Diddens, C. J. Gorter, and M. J. Steenland, Physica **21**, 117 (1955).
[6] R. C. Sapp and C. M. Schroeder, Bull. Am. Phys. Soc. **1**, 91 (1956).
[7] R. V. Jones, W. Dobrowolski, and C. D. Jeffries, Phys. Rev. **102**, 738 (1956).
[8] J. M. Baker, B. Bleaney, P. M. Llewellyn, and P. F. D. Shaw, Proc. Phys. Soc. (London) **69A**, 353 (1956).
[9] Since observed by S. Tanaka, M. Furukawa, S. Iwata, M. Yagi, H. Amano, and T. Mikumo, J. Phys. Soc. Japan **15**, 1547 (1960) and F. S. Houck and J. M. Miller, Phys. Rev. **123**, 231 (1961).
[10] E. W. Backofen and R. H. Herber, Phys. Rev. **97**, 743 (1955).

sible. As complete separation of nickel and manganese by the ion-exchange methods used here is quite difficult and time consuming, the energy of the bombarding alpha particles was reduced to 30 MeV in order to avoid the production of manganese.

III. THE GAMMA-RAY SPECTRUM

The gamma-ray spectrum of Ni^{56} was observed using a 3-in. by 3-in. NaI(Tl) scintillation spectrometer located in a lead house. The spectrometer was calibrated using nuclides whose gamma-ray energies are well known.[11] The Ni^{56} was separated from any cobalt activities in the source just prior to recording the spectrum. Because the daughter Co^{56} activity appreciably disturbed the high-energy portion of the spectrum after approximately 24 h, the separation of the nickel from its cobalt daughter was repeated daily.

A "point" source of Ni^{56} was mounted axially 10 cm from the front face of the detector. The resulting spectrum (Fig. 1) revealed gamma rays of 0.164±0.003, 0.272±0.004, 0.484±0.004, 0.755±0.003, 0.820±0.003, and 1.57±0.01 MeV. The peak at 0.325 MeV was due to the presence of Cr^{51} in this particular source. The peak at 0.98 MeV was due to the summing in the crystal of the 0.164- and 0.755+0.820-MeV gamma rays, and that at 1.09 MeV was due to the summing of the 0.272- and the 0.820-MeV gamma rays. The source was moved to a point 2.4 cm from the detector and the curve in Fig. 2(a) was obtained. Sum peaks appeared at 0.65, 0.98, 1.09, 1.30, and 1.74 MeV, indicating cascades whose members have energies adding to these values.

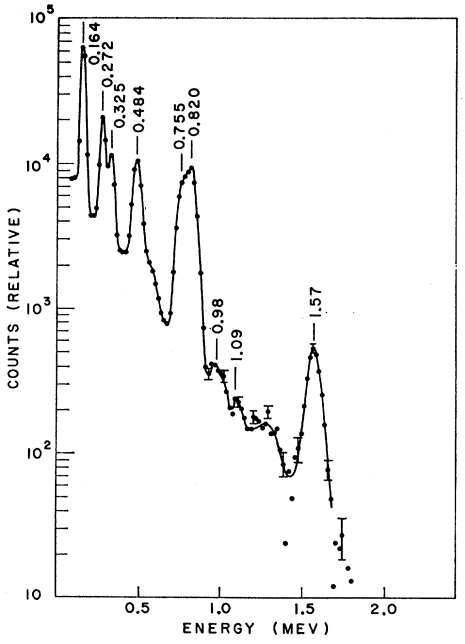

FIG. 1. Ni^{56} single gamma-ray spectrum obtained with a "point" source located axially 10 cm from the face of a 3-in. by 3-in. NaI(Tl) scintillation crystal. The peak at 0.325 MeV was due to a contaminant of Cr^{51}, and that at 1.09 MeV to solid-angle addition in the crystal of gamma rays of 0.272 and 0.820 MeV. The peak at 0.98 MeV in this spectrum was also accounted for by solid-angle addition of the 0.164- and 0.820-MeV gamma rays.

[11] Use was made of Ce^{144}—Pr^{144} (0.134, 1.49, and 2.18 MeV), Na^{22} (0.511 and 1.274 MeV), Cs^{137} (0.662 MeV), Co^{60} (1.173 and 1.333 MeV), and ThC″ (Tl^{208}) (2.614 MeV).

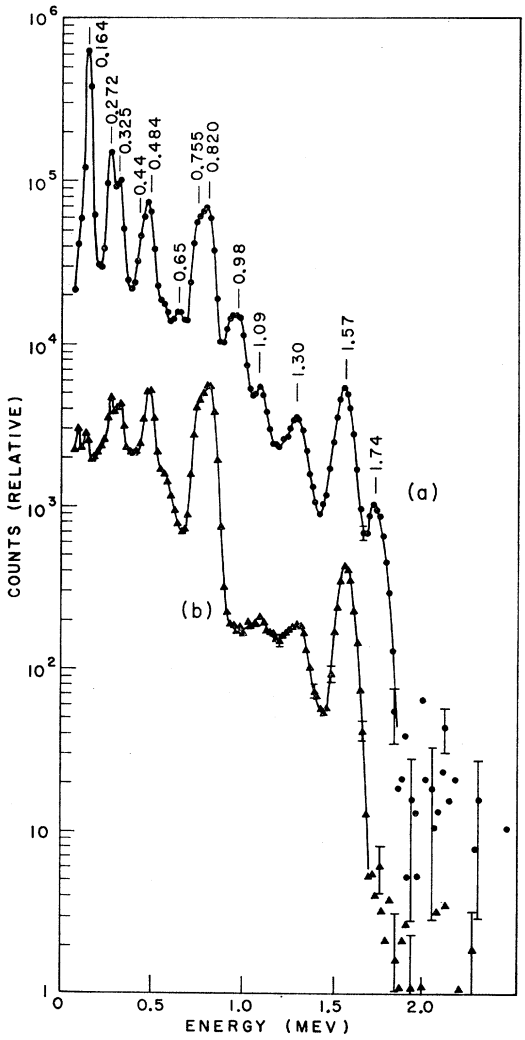

FIG. 2. Ni^{56} single gamma-ray spectra obtained with a "point" source located axially 2.4 cm from the face of a 3-in. by 3-in. NaI(Tl) scintillation crystal. (a) With no absorber, sum peaks of 0.65 (0.164 and 0.484), 0.98 (0.164 and 0.755+0.820 double peak), 1.09 (0.272 and 0.820), 1.30 (0.484 and 0.820), and 1.74 (0.164 and 1.57) MeV appeared. A broadening of the low-energy side of the 0.484-MeV peak indicated summing of the 0.164- and 0.272-MeV gamma rays (0.44 MeV). (b) Upon insertion of 0.32 cm of lead, the sum peaks disappeared. The peak at 0.325 MeV was due to a Cr^{51} contaminant.

Insertion of 0.32 cm of lead between the source and detector [Fig. 2(b)] produced (within statistical error) complete disappearance of the 0.65 (0.164 and 0.484)-, the 0.98 (0.164 and 0.755+0.820)-, and the 1.75 (0.164 and 1.57)-MeV peaks. The 1.09 (0.272 and 0.820)- and

1.30 (0.484 and 0.820)-MeV peaks were also reduced, indicating that they consisted primarily of solid-angle addition of the cascading gamma rays within the detector.

The low-energy portion of the Ni^{56} gamma-ray spectrum was investigated by observing the gamma rays with a NaI(Tl) crystal $\frac{1}{2}$ in. thick by 1 in. in diameter as shown in Fig. 3. This figure also contains the resulting spectrum. No gamma rays were observed between the x-ray energy of 7 keV and 0.164 MeV. The slight rise at 0.06 MeV was part of the room background, and the shoulder at 0.10 MeV was due to the backscattering of the 0.164-MeV gamma ray.

The relative intensities of the gamma rays obtained from analysis of representative spectra of the type shown are presented in Table I. Analysis was performed in the usual manner by obtaining single-gamma-ray spectra

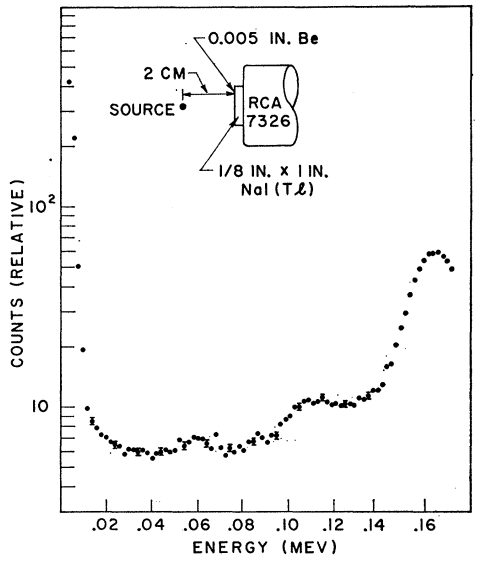

FIG. 3. Low-energy gamma-ray spectrum of Ni^{56}. The shoulder at 0.10 MeV was due to backscattering of the 0.164-MeV gamma ray. The rise at 0.06 MeV was part of the room background.

under conditions identical to those of the experiment and performing successive subtractions starting at the high-energy end of the spectra.

IV. GAMMA GAMMA COINCIDENCE MEASUREMENTS

Gamma-gamma coincidence spectra were measured using a fast-slow coincidence circuit with a resolving time of about 35 nsec. A $1\frac{1}{2}$-in. by $1\frac{1}{2}$-in. NaI(Tl) scintillation spectrometer was used as an analyzing detector and a 3-in. by 3-in. NaI(Tl) scintillation spectrometer was used as a discriminating detector. As shown in Fig. 4, the detectors were shielded from each other and placed 5 and 10 cm, respectively, from a source mounted in a small Teflon cup. The spectrum in coincidence with each of the major gamma rays identified in the singles spectra was measured. Figure 5 shows the settings for the differential discriminator used in these measurements. The results are shown in Figs. 6 and 7. For clarity the curves have been corrected for pulses appearing in the discriminator window caused by Compton events of higher energy gamma rays.

TABLE I. Energies and intensities of gamma rays occurring in the decay of Ni^{56}. The values in column (2) were obtained from analysis of spectra of the type shown in Figs. 1 and 2(b). The values in column (3) were obtained from the spectrum of Fig. 5. Column (4) gives the results of gamma-gamma coincidence data.

Gamma-ray (MeV)	Intensity[a]		
(1)	(2)	(3)	(4)
0.164±0.003	95.2±15.2	104.7±10.5	99.3±6.6
0.272±0.004	37.8± 6.0	37.7± 2.5	31.5±5.2
0.484±0.004	36.0± 4.4	39.4± 2.6	34.6±2.0
0.755±0.003	49.0± 6.1	50.4± 3.4	48.0±3.2
0.820±0.003	88.6±10.9	85.9± 5.7	84.9±8.3
0.98 ±0.01	<1.9	1.1± 0.4	1.2±0.4
1.30	<0.05	<0.1	<0.1
1.47	<0.2	<0.3	<0.02
1.57 ±0.01	11.4± 1.6	13.0± 0.9	14.1±0.9
1.74	···	<0.3	<0.01

[a] Intensities relative to 100 decays $[I(0.820)+I(0.98)+I(1.57)=100]$. See Fig. 14.

The relative intensities of the gamma rays obtained from these measurements are given in Table I. Analysis of the 0.272-, 0.484-, and 0.755-gamma coincidence curves showed the existence of a real 0.98-MeV gamma ray with an intensity of 1.2±0.4 per 100 decays. The 0.164- and 0.272-gamma coincidence data gave an upper limit of 0.1 for the intensity of the 1.30-MeV transition, and the 0.272-gamma data gave a limit of 0.02 for the 1.47-MeV transition. The data were consistent with an upper limit of 0.01 for the fractional intensity of any positron emission as evidenced by the absence of annihilation radiation.

The decay scheme in Fig. 14 was constructed from these results. It should be noted that the absence of the 1.30- and 1.47-MeV "crossover" gamma rays allowed reversal of the order of several cascades. In addition, the data did not rule out the possibility of reversing the entire level sequence. Thus, the decay scheme constructed from the gamma-ray data above was not

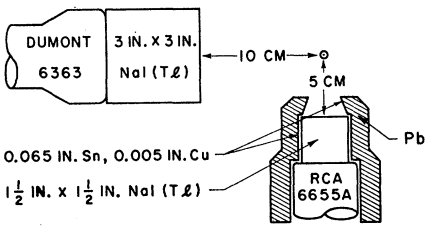

FIG. 4. Geometry for the gamma-gamma coincidence measurements. The 3-in. by 3-in. spectrometer was used as the discriminating detector, and the $1\frac{1}{2}$-in by $1\frac{1}{2}$-in. spectrometer was used for feeding the pulse-height analyzer.

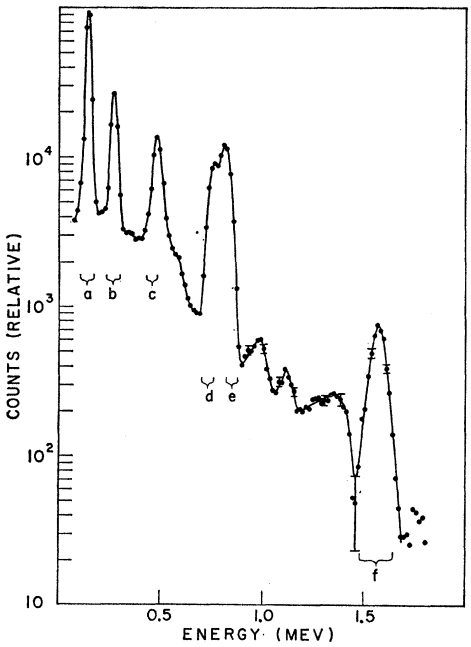

FIG. 5. Single gamma-ray spectrum obtained with the 3-in. by 3-in. spectrometer in the coincidence geometry showing the settings of the differential-discriminator window used in obtaining the spectra of Figs. 6 and 7. Note the absence of the 0.325-MeV peak in this spectrum Gamma-ray intensities obtained from analysis of this curve are included in Table I.

unique. Because detection of the missing "crossover" gamma rays would determine the order of the 0.272–0.484-MeV cascade, several attempts were made to locate them. The detectors were placed in close geometry at 180° and the 0.272- and the 0.484-gamma coincidence spectra were measured with lead absorbers in front of the crystals. Figure 8 shows the results of these measurements. In each case, all counts above 1.0 MeV corresponded to solid-angle addition of the 0.820- and 0.484- or 0.272-MeV gamma rays within the detector. Thus, no conclusive results could be obtained from these data.

A three-crystal pair spectrometer was used in a further attempt to detect the missing gamma rays. However, the available sources were not strong enough to yield conclusive results.

V. DELAYED COINCIDENCE MEASUREMENTS

Measurement of the half lives of the excited states of Co^{56} was performed in order to obtain both an absolute measurement of the transition probability and information concerning the ordering in time of the gamma rays in the various cascades. A coincidence circuit with a time-to-pulse-height converter output similar to that developed by Jones and Warren[12,13] was used. The resolving time of the circuit was about 2 nsec. A 3-in. by 3-in. NaI(Tl) scintillation crystal mounted on an RCA 7046 photomultiplier tube was used for detecting the higher energy gamma ray in the cascade, and a $\frac{1}{2}$-in. by $1\frac{1}{2}$-in. NaI(Tl) scintillation crystal mounted on an RCA 6810A photomultiplier tube was used for detecting the lower energy ones. The detectors were placed with their axes coinciding. The output of the time-to-pulse-height converter was fed into a 256-channel pulse-height analyzer, and the prompt position was adjusted so that it appeared at about one-half of the maximum pulse height. In this way the ordering of the gamma rays was determined directly by observing whether the decay appeared above or below the "prompt" pulse height.

Calibration of the circuit was accomplished by recording a prompt coincidence spectrum with different lengths of RG 63/U delay cable inserted in the two sides of the circuit. The two gamma rays of Y^{88}, which cascade through the 0.1-psec 1.85-MeV state in Sr^{88},[14] provided the prompt coincidences in these experiments.

The 1.57–0.164-MeV cascade was used for the meas-

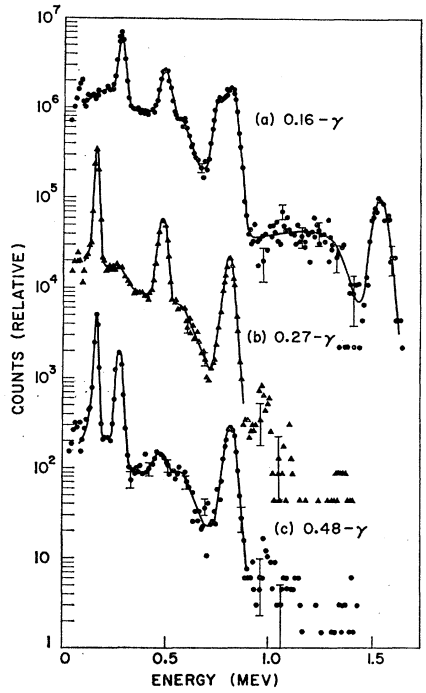

FIG. 6. Gamma-gamma coincidence spectra. Curve (a) shows the spectrum in coincidence with the 0.164-MeV gamma ray. The spectrum is practically identical to the single gamma-ray spectrum when its 0.164-MeV gamma ray is deleted. Curve (b) is the spectrum in coincidence with the 0.272-MeV gamma ray, and curve (c) shows the spectrum in coincidence with the 0.484-MeV gamma ray. The spectra have been corrected for pulses originating with Compton events of higher energy gamma rays and appearing in the differential-discriminator window. In curves (b) and (c), the counts around 1.0 MeV were due to the 0.98-MeV gamma ray and to the summing of 0.164- and 0.820-MeV gamma rays. The counts at higher energies were due to summing. The small peak in curve (c) at about 0.45 MeV was due to the addition of the 0.164- and 0.272-MeV gamma rays in the crystal.

[12] G. Jones and J. B. Warren, J. Sci. Instr. **33**, 429 (1956).
[13] G. Jones, J. Sci. Instr. **37**, 318 (1960).
[14] R. C. Helm, Phys. Rev. **104**, 1466 (1956).

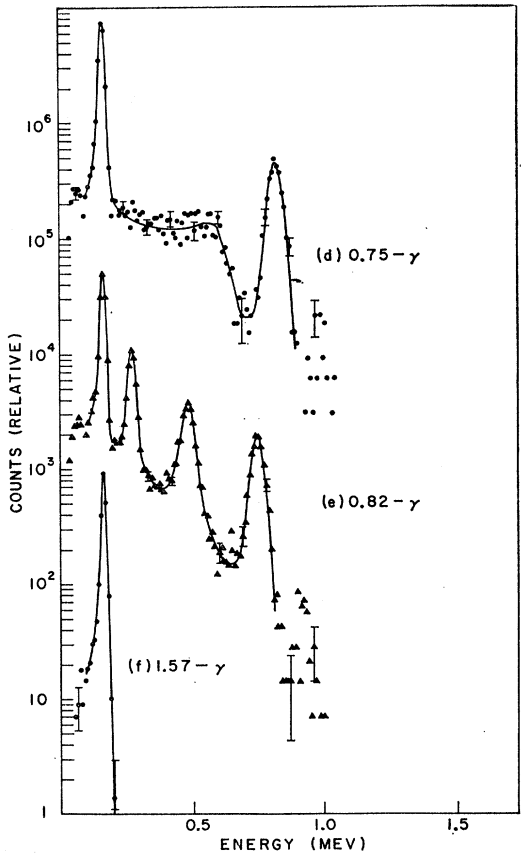

FIG. 7. Gamma-gamma coincidence spectra. Curve (d) is the spectrum in coincidence with the 0.755-MeV gamma ray. The number of counts around 1.0 MeV was larger than would be expected from the summing of the 0.164- and 0.820-MeV gamma rays, indicating the presence of an 0.98-MeV gamma ray. Curve (e) is the spectrum in coincidence with the 0.820-MeV gamma ray. In this case, the number of counts around 1.0 MeV was consistent with the number expected from the summing of the 0.164- and 0.755-MeV gamma rays. Curve (f) is the spectrum in coincidence with the 1.57-MeV gamma ray. With the exception of chance coincidences, no counts were observed above the 0.164-MeV peak. All spectra have been corrected for pulses caused by Compton events of higher energy gamma rays which appeared in the window of the differential discriminator.

urement of the half-life of the 0.164-MeV level. The resulting curve is shown in Fig. 9 along with the "prompt" curve. Analysis by the method of centroid shift[15,16] gave an upper limit of 0.1 nsec for this half-life. The 0.484–0.820-MeV cascade was used to determine the half-life of the 0.984-MeV state. The resulting curves are presented in Fig. 10. An upper limit of 0.1 nsec was also found for the half-life of this level.

Examination of the 0.272–0.484-MeV coincidences showed that the 0.484-MeV gamma ray was delayed with a half-life of 1.61±0.10 nsec. The delayed-coincidence and "prompt" curves are presented in Fig. 11(a). The data were analyzed by fitting an exponential decay to the tail of the delayed-coincidence curve by the

[15] Z. Bay, Phys. Rev. **77**, 419 (1950).
[16] J. D. Newton, Phys. Rev. **78**, 490 (1950).

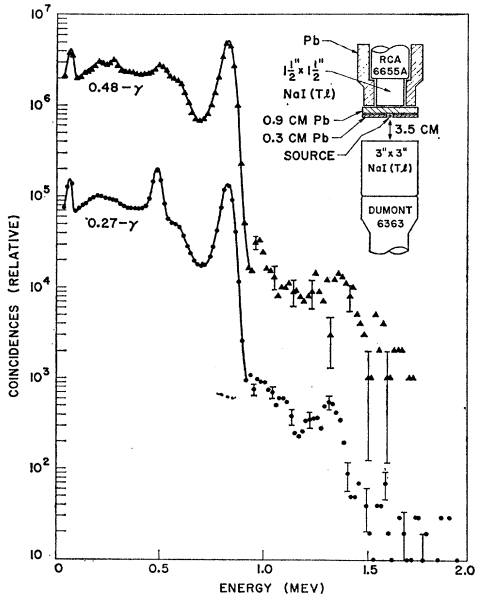

FIG. 8. 0.48- and 0.27-MeV-gamma coincidence spectra taken at 180° with poor geometry. No corrections have been made to the data. In both spectra, all counts above 1.0 MeV corresponded, within experimental error, to addition within the crystal of 0.820- and 0.272- or 0.484-MeV gamma rays.

method of least squares. The half-life obtained using the method of centroid shift was 1.27±0.12 nsec. Figures 11(b) and 11(c) give the results of 0.272–0.820- and 0.272–0.164-MeV delayed-coincidence measurements, taken to determine the order of the other gamma rays. The results showed that the 0.272-MeV gamma ray precedes both the 0.820- and the 0.164-MeV transitions. With this additional information, we concluded that the level scheme of Fig. 14 is correct.

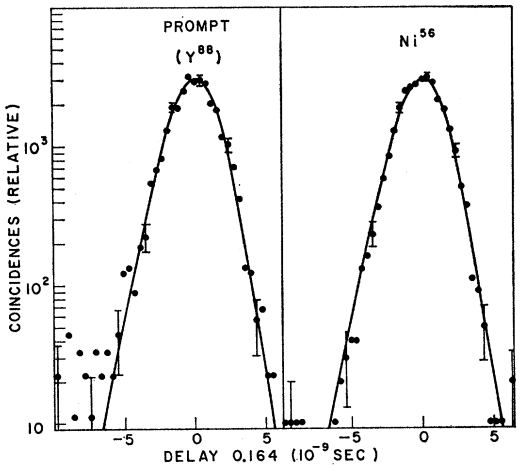

FIG. 9. Delayed-coincidence curve for the 1.57–0.164-MeV gamma-ray cascade. Identical solid lines have been superimposed on both the prompt- and delayed-coincidence curves. The areas of the two curves have been normalized. The method of centroid shift gave an upper limit of 0.1 nsec for the half-life of the intermediate level at 0.164 MeV.

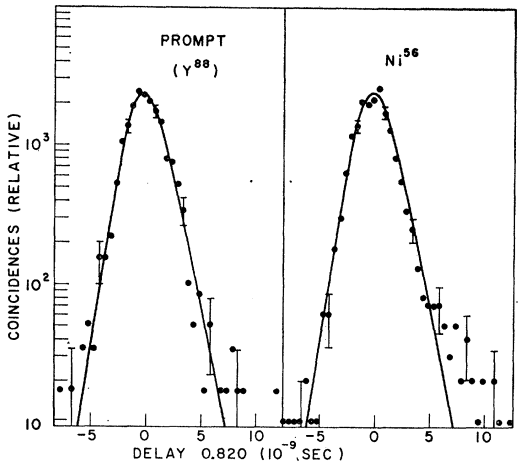

FIG. 10. Delayed-coincidence curve for the 0.484–0.820-MeV gamma-ray cascade. Identical solid lines have been superimposed on both the prompt- and delayed-coincidence curves. The areas of the two curves have been normalized. The method of centroid shift gave an upper limit of 0.1 nsec for the half-life of the intermediate level at 0.984 MeV.

VI. ANGULAR-CORRELATION MEASUREMENTS

The angular correlation of all gamma-ray cascades shown in the decay scheme were measured using the same basic electronic equipment as for the gamma-gamma coincidence measurements. However, the memory of the 256-channel pulse-height analyzer was altered so that it recorded four 64-channel spectra on a time-sharing basis, so that the coincidences involving each of four gamma rays could be recorded at the same time by using four single-channel discriminators. The 3-in. by 3-in. NaI(Tl) detector was used as a stationary, discriminating detector, while the $1\frac{1}{2}$-in. by $1\frac{1}{2}$-in. NaI(Tl) detector was used as a movable, analyzing detector. The 1.57-, 0.820-, 0.484-, and 0.755+0.820-MeV gamma-ray photopeaks (see Fig. 5) were selected in the discriminating single-channel analyzers and coincidence spectra were obtained at angles of 90°, 120°, 150°, and 180°. A total of thirteen separate measurements of 30 min each were made alternately at each angle in order to cancel out the effect of drifts in the electronic equipment. Each spectrum was analyzed separately in the conventional manner to eliminate contributions under the photopeaks from Compton events in the detectors from higher energy radiations.

The data were fit to the correlation function

$$W'(\theta)=1+A_2'P_2(\cos\theta)+A_4'P_4(\cos\theta)$$

by the method of Rose.[17] The resulting curves are presented in Figs. 12 and 13. The correlation functions were corrected for the effects of the finite resolution of the detectors with the aid of the calculations of Stanford and Rivers,[18] and the resulting coefficients A_2 and A_4 are collected in Table II.

[17] M. E. Rose, Phys. Rev. **91**, 610 (1953).

[18] A. L. Stanford, Jr., and W. K. Rivers, Jr., Rev. Sci. Instr. **30**, 719 (1959).

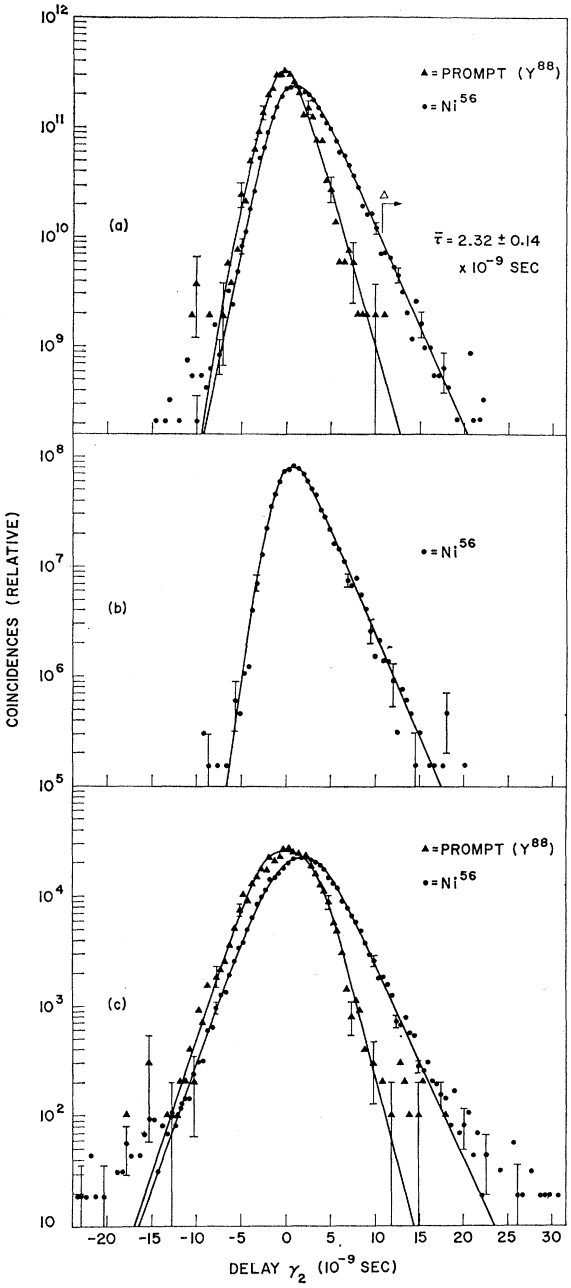

FIG. 11. Delayed-coincidence curves for (a) 0.272–0.484-MeV, (b) 0.272–0.820-MeV, and (c) 0.272–0.164-MeV gamma-ray cascades. The areas of the prompt- and delayed-coincidence curves in the first and third graphs have been normalized. A fit of the data to the right of Δ in curve (a) by the method of least squares yielded a half-life of 1.61±0.10 nsec for the 1.47-MeV level. The right-hand side of each of the solid curves through the delayed-coincidence data was drawn with a slope corresponding to this value. The exponential fall in the direction of positive delays for gamma ray No. 2 in each case indicated that the 0.272-MeV gamma ray precedes those of 0.484, 0.820, and 0.164 MeV. The surplus counts at large delays in curve (c) were due to electronic difficulties encountered when small pulses from each detector were used. These difficulties did not affect the results, however.

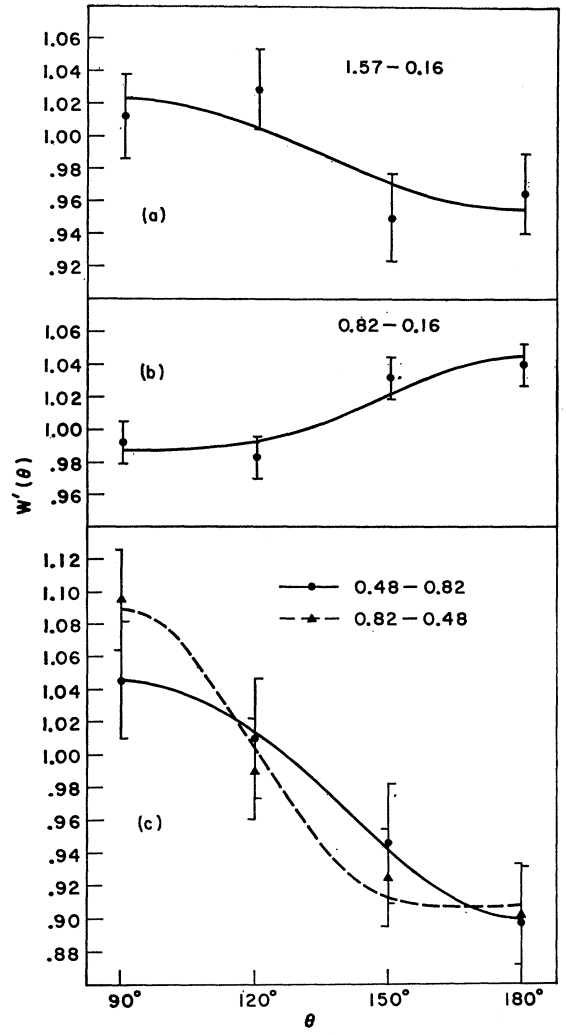

FIG. 12. (a) Angular correlation of the 1.57–0.164-MeV cascade. The solid line is the result of a least-squares fit to the function $W'(\theta)=1-(0.045\pm0.034)P_2(\cos\theta)+(0.001\pm0.042)P_4(\cos\theta)$. (b) Angular correlation of the 0.820–0.164-MeV cascade. The solid line is the result of a least squares fit to the function $W'(\theta)=1+(0.034\pm0.014)P_2+(0.010\pm0.019)P_4$. (c) Angular correlation of the 0.484–0.820-MeV cascade. For the 0.484-gamma coincidence measurement, the least-squares fit yielded $W'(\theta)=1-(0.141\pm0.030)P_2+(0.049\pm0.037)P_4$. For the 0.820-gamma coincidence measurement, the least-squares fit yielded $W'(\theta)=1-(0.093\pm0.037)P_2-(0.007\pm0.047)P_4$. In all cases, the error bars correspond to the root-mean-square errors.

VI. HALF-LIFE OF THE Ni^{56} DECAY

The half-life of the decay of the ground state of Ni^{56} was determined by following the intensities of the 0.164- and 0.272-MeV gamma rays for 17 days. Nine spectra were taken during that time in a fixed geometry. The room background and the contributions due to Compton events of higher energy gamma rays were subtracted from each spectrum. A least-squares fit to the data gave values of 6.10 ± 0.02 and 6.09 ± 0.04 days, respectively.

TABLE II. Angular-correlation coefficients for the gamma-gamma cascades in the decay of Ni^{56}. Corrections for the effect of finite resolution have been made using the curves of Stanford and Rivers.[a]

Gamma-gamma cascade	A_2	A_4	Consistent sequences	Consistent scheme of Table V
1.57 –0.164	-0.049 ± 0.037	0.001 ± 0.057	$1(Q)3(D,Q)4$[b]	1–5
0.820–0.164	0.038 ± 0.016	0.014 ± 0.026	$2(D,Q)3(D,Q)4$	1, 3, 4
			$1(Q)3(D,Q)4$[b]	2, 5
0.755–0.820[c]	0.082 ± 0.042	-0.019 ± 0.062	$1(D,Q)2(D,Q)3$	1, 3, 4
			$1(D,Q)1(Q)3$	2, 5
0.755–0.820[d]	0.116 ± 0.051	-0.050 ± 0.077	$1(D,Q)2(D,Q)3$	1, 3, 4
			$1(D,Q)1(Q)3$[b]	2, 5
0.484–0.820[e]	-0.153 ± 0.033	0.064 ± 0.048	$2(D,Q)2(D,Q)3$	1, 3, 4
			$1(D,Q)2(D,Q)3$	1, 3, 4
			$0(Q)2(D,Q)3$[b,f]	1, 3, 4
0.484–0.820[e]	-0.101 ± 0.040	-0.009 ± 0.060	$2(D,Q)2(D,Q)3$	1, 3, 4
			$1(D,Q)2(D,Q)3$	1, 3, 4
			$2(D,Q)1(Q)3$[b]	2, 5
			$1(D,Q)1(Q)3$[b]	2, 5
			$0(Q)2(D,Q)3$[b]	1, 3, 4
			$0(D)1(Q)3$[b]	2, 5
0.272–0.484	0.053 ± 0.022		$1(D,Q)2(D,Q)2$	1, 3, 4
			$1(D,Q)2(D,Q)1$	2, 5
			$1(D,Q)1(D,Q)2$	1, 3, 4
			$1(D,Q)1(D,Q)1$	2, 5

[a] A. L. Stanford, Jr., and W. K. Rivers, Jr., Rev. Sci. Instr. 30, 719 (1959).
[b] In the theoretical computations, use was made of M. Ferentz and N. Rosenzweig, *Tables of F Coefficients*, Argonne National Laboratory Report ANL-5324 (U. S. Government Printing Office, Washington, 1955).
[c] From 0.820-gamma coincidences.
[d] From (0.755 +0.820)-gamma coincidences.
[e] From 0.484-gamma coincidences.
[f] Consistency with A_4 requires two standard deviations.

VII. INTERPRETATION

From the gamma-ray intensities and the half-life measurements, limitations on the spins and parities of the excited states of Co^{56} were deduced and compared

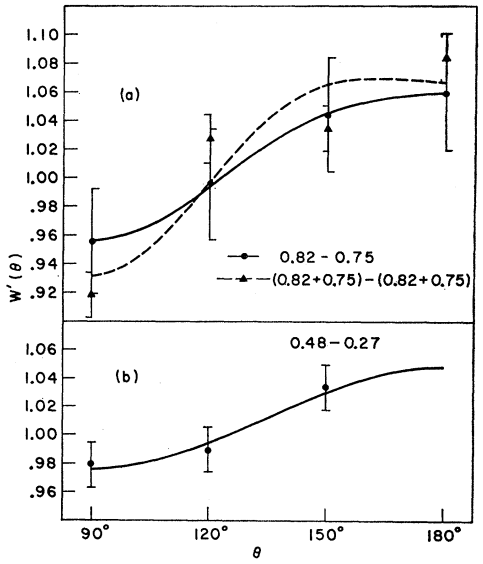

FIG. 13. (a) Angular correlation for the 0.755–0.820-MeV cascade. Least-squares fit was made by $W'(\theta)=1+(0.075\pm0.038)\times P_2(\cos\theta)-(0.015\pm0.049)P_4(\cos\theta)$ for the 0.820-gamma coincidence measurement, and by $W'(\theta)=1+(0.107\pm0.047)P_2-(0.038\pm0.059)P_4$ for the (0.820+0.755)-gamma coincidence measurement. (b) Angular correlation for the 0.484–0.272-MeV cascade. Because of experimental difficulties at 180°, that point was not used. Least-squares fit could, therefore, be only to the function $W'(\theta)=1+(0.049\pm0.020)P_2$.

TABLE III. Weisskopf single-particle estimates for the gamma-ray half-lives (in seconds) of the transitions observed in Co^{56}.[a] A nuclear radius parameter of 1.2×10^{-13} cm was used.

Gamma ray (MeV)	Multipolarity						
	$M1$	$E1$	$M2$	$E2$	$M3$	$E3$	Experiment
0.164	5.08×10^{-12}	1.045×10^{-13}	1.80×10^{-5}	3.68×10^{-7}	96.7	1.98	$\leq10^{-10}$
0.272	1.11×10^{-12}	2.30×10^{-14}	1.43×10^{-6}	2.94×10^{-8}			
0.484	1.98×10^{-13}	4.07×10^{-15}	8.06×10^{-8}	1.65×10^{-9}	4.97×10^{-2}	1.02×10^{-3}	$(1.61\pm0.10)\times10^{-9}$
0.755	5.21×10^{-14}	1.07×10^{-15}	8.71×10^{-9}	1.79×10^{-10}	2.20×10^{-3}	4.51×10^{-5}	
0.820	4.06×10^{-14}	8.38×10^{-16}	5.77×10^{-9}	1.18×10^{-10}	1.24×10^{-3}	2.54×10^{-5}	$\leq10^{-10}$
0.98	2.36×10^{-14}	4.86×10^{-16}	2.34×10^{-9}	4.80×10^{-11}	3.50×10^{-4}	7.15×10^{-6}	
1.57	5.79×10^{-15}	1.19×10^{-16}	2.24×10^{-10}	4.59×10^{-12}			

[a] Computed with the aid of G. J. Nijgh, A. H. Wapstra, and R. van Lieshout, *Nuclear Spectroscopy Tables* (Interscience Publishers, Inc., New York, 1959), pp. 71–4.

with the results of the angular correlation measurements. The intensity balance of the gamma rays in Co^{56} indicated that the beta decay of Ni^{56} proceeds primarily to the 1.74-MeV level. Because Ni^{56} is an even-even nucleus, its ground state was assumed to be 0^+. Therefore, the 1.74-MeV level should have a spin close to zero. Everling *et al.* have estimated the total decay energy of Ni^{56} to be 2.1 MeV on the basis of systematics. Talmi[20] has calculated a value of 1.92 MeV for this energy. From these energies and the half-life for the beta decay of 6.10 days, the log ft value was estimated to be 4.3 or 3.6, respectively.[21] These values indicated that the decay is allowed. Now, allowed spin-zero-to-zero transitions cannot be of the Gamow-Teller type. On the other hand, Fermi-type transitions are expected to be sharply hindered when isospin is not conserved,[22] as it is not in this decay. Thus, the spin of the 1.74-MeV level is probably 1^+ if the estimates of the total decay energy are reasonably correct. Further evidence for the allowed nature of the beta decay was found in the upper limit of 0.01 per decay for the relative intensity of positron emission,[1] which limits the possible positron energy to less than 0.25 MeV,[21] and, thus, the total energy to less than 3.0 MeV. An upper limit on the log ft value of 5.3 is then implied.[21] It should be noted that the expected forbiddenness of the zero-to-zero transitions would allow an assignment of spin zero to some of the lower levels.

From the gross features of the decay scheme certain restrictions could be set on the spins of the 0.164-, 0.984-, and 1.47-MeV levels of Co^{56}. With the exception of the weak 0.98-MeV gamma ray, the only observed transition to the ground state was the one from the 0.164-MeV level. Hence, provided the transition matrix elements are not accidentally small, the spin difference between the 0.984-, 1.47-, and 1.74-MeV levels and the ground state must be larger than that between these levels and the 0.164-MeV level. The ground state is known to be 4^+.[7,8] Since the 1.74-MeV level is most likely 1^+ (or zero), the spin of the 0.164-MeV level was expected to be equal to or less than three, and that of the 0.984- and 1.47-MeV states zero, one, or two.

From a comparison of the half-life of the 0.164-MeV transition (upper limit 0.1 nsec) with the Weisskopf single-particle estimates (see Table III), we concluded that the 0.164-MeV transition is most likely $E1$ or $M1$. From the intensity balance of the gamma rays, it appeared that there is more than a 90% chance that the internal-conversion coefficient for this transition is less than 0.07, which is in agreement with the proposed dipole character of this transition (see Table IV). The 0.164-MeV level must then have spin three.

On this basis the 1.57-MeV gamma ray was, thus, taken to be a quadrupole transition. Comparison of the experimental relative transition rates for the 0.272- and 1.57-MeV gamma rays with the single-particle estimates indicated that, if the 1.57-MeV gamma rays is $M2$, the 0.272-MeV gamma ray must be $M1$ or if the 1.57-MeV gamma ray is $E2$, the 0.272-MeV gamma ray can be either $M1$ or $E1$. (An assignment was assumed to be reasonable if experimental and single-particle relative transition rates agreed to within a fact or of 100.[23])

TABLE IV. Theoretical internal-conversion coefficients for the 0.164-MeV transition for $L=1$, 2, and 3.[a]

Multipolarity	Conversion coefficient
$M1$	0.0105
$E1$	0.0097
$M2$	0.076
$E2$	0.072
$M3$	0.50
$E3$	0.50
Experimental	≤0.07

[a] M. E. Rose, *Internal Conversion Coefficients* (Interscience Publishers, Inc., New York, 1958), pp. 6, 7.

[19] F. Everling, N. B. Gove, and R. van Lieshout, in *Beta-Disintegration Energy Charts* (Nuclear Data Project, National Academy of Sciences–National Research Council, Washington, D. C., 1962).

[20] I. Talmi, Phys. Rev. **107**, 326L (1957) and private communication.

[21] G. J. Nijgh, A. H. Wapstra, and R. Van Lieshout, in *Nuclear Spectroscopy Tables* (Interscience Publishers, Inc., New York, 1959.

[22] S. D. Bloom, L. G. Mann, and J. A. Miskel, Phys. Rev. **125**, 2021 (1962); see also W. M. McDonald, in *Nuclear Spectroscopy*, edited by F. Ajzenberg-Selove (Academic Press Inc., New York, 1960), Vol. B, p. 932 ff.

[23] While the single-particle estimates for the transition rates often deviate by large factors from the actual values, the deviations are always to slower rates (excepting collective $E2$ transitions). Thus, the ratios of the rates should be useful to within a few orders of magnitude. See reference 21 and M. Goldhaber and A. W. Sunyar, in *Beta- and Gamma-Ray Spectrsocopy*, edited by K. Siegbahn (Interscience Publishers, Inc., New York, 1955), chap. XVI (II), pp. 453–67.

TABLE V. Possible combinations of multipolarities for the gamma rays of Co^{56} and the resultant spin assignments for the observed energy levels as deduced from the beta- and gamma-ray transition rates only.

Gamma ray (MeV)	(1)	(2)	(3)	(4)	(5)
1.57	$M2$	$M2$	$E2$	$E2$	$E2$
0.98	$E2$	$M3$	$E2$	$E2$	$E3$
0.820	$E1$	$M2$	$M1$	$M1$	$M2$
0.755	$M1$	$M1$	$M1$	$M1$	$E1$
0.484	$M1$, $E2$	$M1$	$M1$, $E2$	$E1$, $M2$	$M1$
0.272	$M1$	$M1$	$M1$	$E1$	$E1$
0.164	$E1$	$E1$	$M1$	$M1$	$M1$
Level (MeV)	Spin and parity assignments				
1.74	1^+	1^+	1^+	1^+	1^+
1.47	$0, 1, 2^+$	$0, 1, 2^+$	$0, 1, 2^+$	$0, 1, 2^-$	$0, 1, 2^-$
0.984	2^+	1^+	2^+	2^+	1^-
0.164	3^-	3^-	3^+	3^+	3^+
0	4^+	4^+	4^+	4^+	4^+

Thus, the 1.47-MeV level was assumed to have spin zero, one, or two.

The upper limit of 0.1 nsec for the half-life of the 0.984-MeV level is consistent with the 0.820-MeV gamma ray being dipole or quadrupole (see Table III). Comparison of the relative transition rates for the 0.820- and the 0.98-MeV gamma rays with the single-particle estimates indicated the following possibilities: (1) that the 0.820-MeV gamma ray is $M1$ and the 0.98 either $M1$ or $E2$, (2) that the 0.820 is $E1$ and the 0.98 $E2$, or (3) that the 0.820 is $M2$ and the 0.98 either $M3$ or $E3$. In any case, the spin of the 0.984-MeV level could not be zero, but could be one or two.

The measured half-life for the 0.484-MeV transition is consistent with multipolarity two or with forbidden multipolarity one (see Table III). The experimental relative transition rates for the 0.272- and the 0.755-MeV gamma rays are consistent with both transitions being $M1$ or with the 0.272 being $E1$ and the 0.755 being either $M1$ or $E1$. In summary, there are only five consistent combinations of multipolarities for the gamma rays in this decay. They are given in Table V.

The gamma-gamma angular-correlation measurements were interpreted by the methods of Arns and Weidenbeck,[24] and the results are contained in Table II. Quadrupole transitions were assumed to be pure, while dipole transitions were permitted to have admixtures of quadrupole radiation. For the 1.57–0.164-MeV correlation, the data could be fit for a sequence of the form $1(Q)3(D,Q)4$. The amplitude for the quadrupole admixture to the 0.164-MeV transition was found to be between 0.0 and -0.1. Using this amplitude, the 0.820–0.164-MeV correlation was interpreted. The data permitted the sequence $2(D,Q)3(D,Q)4$ with a wide range of quadrupole admixtures for the 0.820-MeV transition. The correlation coefficients for this cascade could also be fit with a sequence $1(Q)3(D,Q)4$; however, the mixing intensity for the 0.164-MeV transition then implied was not consistent with that obtained for the 1.57–0.164-MeV measurement. A spin of two was, therefore, indicated for the 0.984-MeV level, and the sets of spins in columns (2) and (5) of Table V were eliminated.

The 0.755–0.820-MeV correlation was interpreted using the limits placed on the mixing intensity of the 0.820-MeV transition by the above correlations. The data could be fit with either a $1(D,Q)2(D,Q)3$ or a $1(D,Q)1(Q)3$ sequence. Thus, this correlation could not be used to support the elimination of spin one for the 0.984-MeV level. The 0.484–0.820 MeV correlation was also interpreted with the help of the above results. Consistent fits were obtained for the $2(D,Q)2(D,Q)3$, $1(D,Q)2(D,Q)3$, and $0(Q)2(D,Q)3$ sequences for both measurements of this correlation. Sequences with spin one for the 0.984-MeV level were consistent with the data obtained from the 0.484-gamma coincidences, but they did not fit the results of the other measurement of this correlation. The elimination of spin one for the 0.984-MeV level is, therefore, partially supported by these results.

While experimental difficulties made analysis of a 0.272–0.484-MeV correlation unsure, the nonisotropic distribution seemed well outside of experimental error. The spin of the 1.47-MeV level should not then be zero. Analysis showed the correlation to be consistent with the sequences $1(D,Q)2(D,Q)2$, $1(D,Q)2(D,Q)1$, $1(D,Q)1(D,Q)2$, and $1(D,Q)1(D,Q)1$, the first and third agreeing with the results of the other correlations.

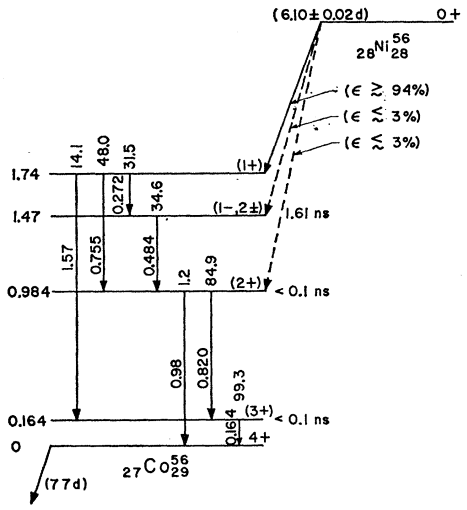

FIG. 14. Decay scheme for Ni^{56}. See text for a discussion of the spin assignments. Upper limits for the gamma rays not shown on the figure were determined to be as follows (see Table I): 1.74-MeV gamma ray <0.01, 1.47-MeV <0.02, 1.30-MeV <0.05. The total decay energy of Ni^{56} to Co^{56} is 2.1 MeV, as inferred from decay systematics (reference 19).

[24] R. G. Arns and M. L. Wiedenbeck, Phys. Rev. **111**, 1633 (1958) and University of Michigan Engineering Research Institute Technical Report 2375-3-T, 1958 (unpublished).

The amount of quadrupole admixture to the dipole transitions, with the exception of the 0.164-MeV transition, varied within wide limits and could not be determined from these measurements. It was noted, however, that the data could be fit for all transitions being pure—i.e., no mixing.

VIII. DISCUSSION

The complete decay scheme is presented in Fig. 14. The spins and parities of the ground state, the 0.984-MeV level, and the 1.74-MeV level were determined with reasonable certainty to be 4^+, 2^+, and 1^+, respectively. The spin of the 0.164-MeV level was found to be three. Since there are no low-lying levels with negative parity in odd-odd nuclei in this region of the periodic table, this level is very probably 3^+. For the 1.47-MeV level the data allowed a spin of one or two. If this level were 1^+, one would expect it to be fed by an allowed beta decay, which was not observed. Provided the allowed beta-decay matrix element for decay to this level is not accidentally small, the 1.47-MeV level is not expected to be 1^+. It could be 1^- or $2^\pm$. Comparison with detailed shell-model predictions will be made in another publication.[25]

The discrepancies between the results of references 1, 3, and 4 and the present work in the gamma rays observed and their intensities is thought to be due to the possible presence of Mn^{52} in the sources used in the previous experiments. Recently, Nelson *et al.*[26] have investigated some of the lower levels of Co^{56} by determining the (p,n) thresholds for Fe^{56}. They found thresholds which they interpreted as levels at 0, 0.162 ± 0.014, 0.189 ± 0.017, 0.229 ± 0.017, and 0.283 ± 0.087 MeV. The lowest excited state identified in their work agrees with the lowest state in ours, indicating that our over-all over-all decay scheme should not be inverted. The remaining three levels could be due to core or multiple-particle excitations which might be excited by a 5.5-MeV proton, but which would not be observed in the beta decay of Ni^{56}. However, Anderson *et al.*[27] have also used the $Fe^{56}(p,n)Co^{56}$ reaction to study the levels of Co^{56}. By using time-of-flight techniques, they observed neutron groups corresponding to states at 0, 0.165, 0.560, 0.825, 0.980, and 1.105 MeV with an error of ±0.015 MeV. The other levels indicated by reference 26 were not found, so that they may well be spurious. The states Mat 0.165 and 0.980 MeV correspond very nicely to levels observed in our work. The other levels are probably high-spin levels not populated in the decay of Ni^{56}.[25]

Ohnuma[28] has recently begun a study of the radioactive decay of Ni^{56}. His preliminary results are in substantial agreement with ours.

A careful measurement of the internal-conversion coefficients for the lower energy transitions would be very useful for checking the spin and parity assignments of the levels of Co^{56}. Our attempts to measure these coefficients were hindered by a nonradioactive substance accompanying the Ni^{56} (probably Ni impurity in the iron target[29]) which made preparation of thin beta-ray sources impossible.

ACKNOWLEDGMENTS

We would like to thank Professor A. de Shalit and Professor I. Talmi for many suggestions concerning the interpretation of our data. Dr. D. J. Horen, Dr. D. Kohler, and Dr. P. Paul contributed helpful suggestions at various stages of the work. Dr. I. Boekelheide helped with taking much of the data, and B. Hoop contributed appreciably to perfection of the chemical techniques for the separation of Ni from Fe and from other reaction products. We are also very grateful to Bart Jones, Peter McWalter, and the crew of the 60-in. cyclotron of the Crocker Radiation Laboratory of the University of California for preparation of our sources. Dr. J. R. Wilkinson sent us his unpublished results, and Dr. Ohnuma sent his results before publication, and for this we thank them. One of us (DOW) is very grateful to the Missile and Space Division of the Lockheed Aircraft Corporation, Palo Alto, California, for partial support during the course of most of this work.

[25] D. O. Wells (to be published).
[26] J. W. Nelson, H. S. Plendl, and R. H. Davis, Phys. Rev. **125**, 2005 (1962).
[27] J. D. Anderson, C. Wong, and J. McClure, Nucl. Phys. **36**, 161 (1962).
[28] H. Ohnuma (private communication).
[29] C. Jenkins (private communication).